

Plane-wave scattering by a set of perfectly conducting circular cylinders in the presence of a plane surface

Riccardo Borghi, Franco Gori, and Massimo Santarsiero

Dipartimento di Fisica, Università La Sapienza, Piazzale Aldo Moro 2, 00185 Rome, Italy

Fabrizio Frezza and Giuseppe Schettini

Dipartimento di Ingegneria Elettronica, Università La Sapienza, Via Eudossiana 18, 00184 Rome, Italy

Received January 2, 1996; revised manuscript received July 3, 1996; accepted July 5, 1996

A general approach is presented for treating the two-dimensional scattering of a plane wave by an arbitrary configuration of perfectly conducting circular cylinders in front of a plane surface with general reflection properties. The method exploits the angular spectrum representation of cylindrical waves and turns out to be fairly efficient, as demonstrated by a number of examples. Our approach seems promising for several applications both in optics and in microwaves. © 1996 Optical Society of America.

1. INTRODUCTION

The problem of scattering of a plane wave by sets of perfectly conducting indefinite circular cylinders with parallel axes in an isotropic and homogeneous medium has been treated by various authors. The case of an infinite grating of circular cylinders was studied in Refs. 1 and 2. Some numerical data on transmission coefficients were obtained in Ref. 3. The limiting case of wires, i.e., cylinders whose radii are negligible with respect to the wavelength, was considered for an infinite grid by Wait,⁴ and scattering from a finite number N of parallel conducting wires was studied in Refs. 5–7. The case of wires has great practical importance because scatterers of arbitrary shape can be simulated, and even built, by means of a suitable wire grid.⁵ Some rules of thumb have been given to optimize the dimensions of the equivalent grid.^{8,9} For cylindrical structures with radii comparable with or larger than the wavelength the wire approximation cannot be used, and one must resort to a rigorous approach. The case of two cylinders was treated in Refs. 10–12. The multiple-scattering approach was introduced in Refs. 13 and 14, while in Ref. 15 the problem of N conducting circular cylinders in free space was solved. A comprehensive review of this problem is presented in Ref. 16. Numerical solutions for two-dimensional scattering by structures of arbitrary shape are presented in Refs. 17–20. Finally, the problem has been tackled in Ref. 10 for the case of dielectric cylinders, in Ref. 21 for application to parallel glass fibers, and in Ref. 22 with a multiple-scattering approach.

In the presence of a plane interface, owing to the various geometrical features of the interacting waves and bodies, the solution of the scattering problem is a more difficult task. However, several results can be found in the literature for particular cases. For example, an infinite wire grid parallel to the interface was treated by

Wait for cases of both a perfectly conducting plane²³ and a vacuum-dielectric interface.²⁴ Furthermore, for the case of a single cylinder in front of an interface, the problem has been approached with various techniques.^{25–30} When the surface coincides with the interface between vacuum and a dielectric homogeneous medium or when it is a real conducting plane, solutions are available also for noncylindrical objects.^{31–34} In addition, partially buried scatterers have recently been considered.^{35,36}

Among the several applications of gratings in free space we quote Refs. 37–39, where the grids are used as couplers and mirrors. A wide range of applications for conducting or dielectric grids is represented by the simulation of cylindrical objects.^{40,41} The theory of scattering by cylinders in the presence of an interface has been applied to the detection of defects in the semiconductor industry.^{42,43} Finally, in recent years metallic arrays have been proposed as quasi-optical launchers of lower-hybrid waves for microwave heating of thermonuclear plasmas,^{44–46} as an alternative to the customary waveguide phased arrays.

In Ref. 25 we presented a general technique to solve the plane-wave scattering problem for a perfectly conducting circular cylinder in front of an arbitrary reflecting plane interface for both TM and TE polarization states. Such a technique proved to be fairly efficient and accurate.

In this paper we generalize that analysis to the case of a finite number N of perfectly conducting circular cylinders with possibly different radii. The axes of the cylinders can be arbitrarily placed with respect to the interface. In Section 2 the theoretical analysis is outlined and expressions of the scattered fields are given. The far-field limit is also considered. In Section 3 the convergence problem is treated and numerical results are presented for the far field. Comparisons are made with the results obtained for some particular cases in which alter-

native approaches are used. Our method allows us to deal with reflecting surfaces of general behavior, such as lossy, anisotropic, and multilayered interfaces. It seems particularly efficient in terms of computation time, stability, and reliability of the results.

2. THEORETICAL ANALYSIS

A. General Theory

In Fig. 1 the geometrical layout of the problem is shown: N perfectly conducting circular cylinders with radii a_t ($t = 1, \dots, N$) are placed in front of the reflecting surface. The axis of each cylinder is parallel to the y axis, and the structure is assumed to be infinite along the y direction, so that the problem is reduced to a two-dimensional form. The incident field is a monochromatic plane wave, whose wave vector \mathbf{k}^i lies in the x - z plane. The polarization is said to be TM (with respect to the axis of each cylinder) or E when the electric field is directed along the y axis and TE or H when the magnetic field is axially directed. φ is the angle between the wave vector \mathbf{k}^i and the x axis, and thus \mathbf{k}^i is related to φ through the expressions

$$k_{\parallel}^i = k \sin \varphi, \quad k_{\perp}^i = k \cos \varphi, \quad (1)$$

where the symbols \perp and \parallel refer to the orthogonal and the parallel components, respectively, of a vector with respect to the interface. The presence of the interface is described by the complex reflection coefficient $\Gamma(n_{\parallel})$, where $\mathbf{n} = \mathbf{k}/k$, \mathbf{k} being the wave vector of a plane wave incident on the surface and $k = 2\pi/\lambda$ being the wave number.

In the following, for the sake of brevity, dimensionless coordinates $\xi = kx$, $\zeta = kz$ will be used. Let $\boldsymbol{\rho}_t^0 \equiv (\xi_t^0, \zeta_t^0)$ ($t = 1, \dots, N$) be the position vector of the axis of the t th cylinder in the main reference frame (O, ξ, ζ) (MRF from now on), and $\boldsymbol{\rho}_t \equiv (\xi_t, \zeta_t)$ ($t = 1, \dots, N$) be the typical position vector in the frame centered on that cylinder (RF $_t$ from now on). It is convenient to choose the ζ axis of the MRF lying on the reflecting surface. In the following, $V(\xi, \zeta)$ stands for the component of the electromagnetic field parallel to the

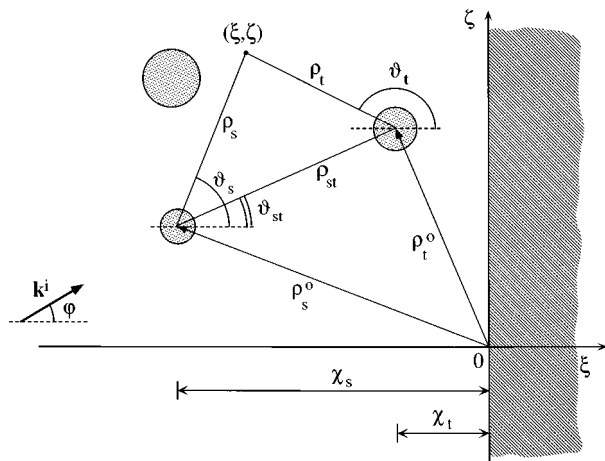


Fig. 1. Geometry of the problem and notation used throughout the paper.

y axis; i.e., $V = E_y$ for TM polarization and $V = H_y$ for TE polarization. By using the same procedure as in Ref. 25, we will express this field as the sum of four contributions; then we will expand each of them in terms of cylindrical functions centered on the origin of each RF $_t$. This will allow the imposition of the boundary conditions on the surface of each cylinder to be satisfied in a simple way. Let us analyze separately the four contributions to the field:

Incident field V_i . The incident field has the form

$$V_i(\xi, \zeta) = V_0 \exp(in_{\perp}^i \xi + in_{\parallel}^i \zeta), \quad (2)$$

where V_0 is the complex amplitude of the incident field in the origin of the MRF. Since $\xi = \xi_t^0 + \xi_t$ and $\zeta = \zeta_t^0 + \zeta_t$ (see Fig. 1), Eq. (2) can be written in the RF $_t$ as

$$\begin{aligned} V_i(\xi, \zeta) &= V_0 \exp(in_{\perp}^i \xi_t^0 + in_{\parallel}^i \zeta_t^0) \exp(in_{\perp}^i \xi_t + in_{\parallel}^i \zeta_t) \\ &= V_0 \exp(in_{\perp}^i \xi_t^0 + in_{\parallel}^i \zeta_t^0) \sum_{m=-\infty}^{+\infty} i^m \\ &\quad \times \exp(-im\varphi) J_m(\rho_t) \exp(im\vartheta_t), \end{aligned} \quad (3)$$

where (ρ_t, ϑ_t) are polar coordinates in the RF $_t$ and use has been made of the expansion of a plane wave in terms of Bessel functions J_m .⁴⁷ We stress that Eq. (3) represents the field associated with the point that has coordinates (ξ, ζ) in the MRF as a function of the coordinates (ξ_t, ζ_t) in the RF $_t$.

Reflected field V_r . The field due to the reflection of V_i by the surface is

$$V_r(\xi, \zeta) = V_0 \Gamma(n_{\parallel}^i) \exp(-in_{\perp}^i \xi + in_{\parallel}^i \zeta). \quad (4)$$

By proceeding in the same way as for the incident field, we obtain

$$\begin{aligned} V_r(\xi, \zeta) &= V_0 \Gamma(n_{\parallel}^i) \exp(-in_{\perp}^i \xi_t^0 + in_{\parallel}^i \zeta_t^0) \\ &\quad \times \exp(-in_{\perp}^i \xi_t + in_{\parallel}^i \zeta_t) \\ &= V_0 \Gamma(n_{\parallel}^i) \exp(-in_{\perp}^i \xi_t^0 + in_{\parallel}^i \zeta_t^0) \\ &\quad \times \sum_{m=-\infty}^{+\infty} i^m \exp(-im\bar{\varphi}) \\ &\quad \times J_m(\rho_t) \exp(im\vartheta_t), \end{aligned} \quad (5)$$

where $\bar{\varphi} = \pi - \varphi$ denotes the angle of propagation of the reflected plane wave.

Diffracted field V_d . This field can be written as the sum of the fields diffracted by each cylinder, which, in turn, is expressed by means of a superposition of cylindrical functions with unknown coefficients c_{sm} . That is,

$$V_d(\xi, \zeta) = V_0 \sum_{s=1}^N \sum_{m=-\infty}^{+\infty} i^m \exp(-im\varphi) c_{sm} CW_m(\xi_s, \zeta_s), \quad (6)$$

where $CW_m(\xi_s, \zeta_s)$ is the cylindrical function²⁵

$$CW_m(\xi_s, \zeta_s) = H_m^{(1)}(\rho_s) \exp(im\vartheta_s) \quad (7)$$

and $H_m^{(1)}$ is the outgoing Hankel function.⁴⁷ By using Graf's formula⁴⁸ we can write all the cylindrical functions relevant to the s th cylinder (with $s \neq t$) in RF $_t$; i.e.,

$$\begin{aligned}
V_d(\xi, \zeta) &= V_0 \sum_{m=-\infty}^{+\infty} i^m \exp(-im\varphi) c_{tm} \text{CW}_m(\xi_t, \zeta_t) \\
&+ V_0 \sum_{\substack{s=1 \\ s \neq t}}^N \sum_{m=-\infty}^{+\infty} i^m \exp(-im\varphi) c_{sm} \\
&\times \exp(im\vartheta_{st}) \sum_{l=-\infty}^{+\infty} (-1)^l H_{m+l}^{(1)}(\rho_{st}) \\
&\times \exp(il\vartheta_{st}) J_l(\rho_t) \exp(-il\vartheta_t), \quad (8)
\end{aligned}$$

where ρ_{st} and ϑ_{st} are shown in Fig. 1. By interchanging indexes m and l in the double sum, we obtain

$$\begin{aligned}
V_d(\xi, \zeta) &= V_0 \sum_{m=-\infty}^{+\infty} i^m \exp(-im\varphi) c_{tm} \text{CW}_m(\xi_t, \zeta_t) \\
&+ V_0 \sum_{\substack{s=1 \\ s \neq t}}^N \sum_{l=-\infty}^{+\infty} i^l \exp(-il\varphi) c_{sl} \\
&\times \sum_{m=-\infty}^{+\infty} H_{l+m}^{(1)}(\rho_{st}) \exp[i(l+m)\vartheta_{st}] \\
&\times (-1)^m J_m(\rho_t) \exp(-im\vartheta_t); \quad (9)
\end{aligned}$$

taking into account the relation $J_{-m}(x) = (-1)^m J_m(x)$ and replacing m with $-m$ in the last sum, we obtain

$$\begin{aligned}
V_d(\xi, \zeta) &= V_0 \sum_{m=-\infty}^{+\infty} i^m \exp(-im\varphi) c_{tm} \text{CW}_m(\xi_t, \zeta_t) \\
&+ V_0 \sum_{\substack{s=1 \\ s \neq t}}^N \sum_{l=-\infty}^{+\infty} i^l \exp(-il\varphi) c_{sl} \\
&\times \sum_{m=-\infty}^{+\infty} \text{CW}_{l-m}(\xi_{st}, \zeta_{st}) J_m(\rho_t) \exp(im\vartheta_t), \quad (10)
\end{aligned}$$

where (ξ_{st}, ζ_{st}) are Cartesian coordinates corresponding to $(\rho_{st}, \vartheta_{st})$. After some algebra, from Eqs. (7) and (10) it is possible to obtain the more compact form

$$\begin{aligned}
V_d(\xi, \zeta) &= V_0 \sum_{m=-\infty}^{+\infty} J_m(\rho_t) \exp(im\vartheta_t) \sum_{s=1}^N \sum_{l=-\infty}^{+\infty} i^l \\
&\times \exp(-il\varphi) c_{sl} \left[\text{CW}_{l-m}(\xi_{st}, \zeta_{st}) \right. \\
&\times \left. (1 - \delta_{st}) + \delta_{st} \delta_{lm} \frac{H_m^{(1)}(\rho_t)}{J_m(\rho_t)} \right]. \quad (11)
\end{aligned}$$

The interaction between the s th and t th cylinders is contained in the term $\text{CW}_{l-m}(\xi_{st}, \zeta_{st})(1 - \delta_{st})$, which is a consequence of Graf's formula,⁴⁸ giving the expression of a cylindrical wave emitted by the s th cylinder in the RF $_t$. When all cylinders can be considered to be noninteracting, owing to the vanishing of the interaction term, the field (11) reduces to the superposition of N fields evaluated by means of the classical formula for an isolated cylinder.⁴⁹ For example, this happens when the

mutual distances between the cylinders are large enough, owing to the behavior of the Hankel functions.⁵⁰

Diffracted-reflected field V_{dr} . Since the diffracted field V_d has been expanded in terms of cylindrical outgoing waves [see Eq. (6)], but the reflection properties of the plane of discontinuity are generally known for plane incident waves,⁵¹ an expression of V_{dr} may be obtained by using the analytical plane-wave spectrum of CW_m functions.^{25,52} In particular, in Ref. 25 we showed that the field that is due to the reflection of a typical cylindrical wave $\text{CW}_m(\xi_s, \zeta_s)$ by the interface can be written as $\text{RW}_m(2\chi_s - \xi_s, \zeta_s)$, $\text{RW}_m(\xi, \zeta)$ being the function defined as

$$\text{RW}_m(\xi, \zeta) = \frac{1}{2\pi} \int_{-\infty}^{+\infty} \Gamma(n_{\parallel}) F_m(\xi, n_{\parallel}) \exp(in_{\parallel}\zeta) dn_{\parallel}, \quad (12)$$

where $\chi_s = -\xi_s^0$ denotes the distance between the axis of the s th cylinder and the reflecting surface (see Fig. 1) and $F_m(\xi, n_{\parallel})$ is the angular spectrum of the cylindrical function CW_m , defined as

$$F_m(\xi, n_{\parallel}) = \int_{-\infty}^{+\infty} \text{CW}_m(\xi, \zeta) \exp(-in_{\parallel}\zeta) d\zeta. \quad (13)$$

By considering the reflection of each cylindrical wave and summing all the contributions, from Eq. (6) we obtain

$$\begin{aligned}
V_{dr}(\xi, \zeta) &= V_0 \sum_{s=1}^N \sum_{m=-\infty}^{+\infty} i^m \exp(-im\varphi) \\
&\times c_{sm} \text{RW}_m(2\chi_s - \xi_s, \zeta_s). \quad (14)
\end{aligned}$$

Equation (14) shows that the diffracted-reflected field can be thought of as a superposition of the fields diffracted by "image" cylinders centered at the points $(-\xi_s^0, \zeta_s^0)$, for $s = 1, \dots, N$. These fields are modulated by the presence of the interface through the definition of RW_m functions [see Eq. (12)].

Taking into account the explicit expression of the F_m functions,^{25,52} i.e.,

$$\begin{aligned}
F_m(\xi, n_{\parallel}) &= \frac{2 \exp(in_{\perp}\xi)}{n_{\perp}} \exp(-im \arccos n_{\parallel}), \\
n_{\parallel} &\in (-\infty, +\infty), \quad (15)
\end{aligned}$$

we have

$$\begin{aligned}
\text{RW}_m(2\chi_s - \xi_s, \zeta_s) &= \frac{1}{2\pi} \int_{-\infty}^{+\infty} \Gamma(n_{\parallel}) F_m(-2\xi_s^0 - \xi + \xi_s^0, n_{\parallel}) \\
&\times \exp(-in_{\parallel}\zeta_s^0) \exp(in_{\parallel}\zeta) dn_{\parallel} \\
&= \frac{1}{2\pi} \int_{-\infty}^{+\infty} \Gamma(n_{\parallel}) F_m(\chi_s, n_{\parallel}) \\
&\times \exp[in_{\parallel}(\zeta - \zeta_s^0)] \exp(-in_{\perp}\xi) dn_{\parallel}. \quad (16)
\end{aligned}$$

Finally, taking into account that $\xi = \xi_t^0 + \xi_t$, $\zeta = \zeta_t^0 + \zeta_t$ and $\xi_t^0 = -\chi_t$, from Eq. (16) the field due to the reflection of a typical cylindrical wave centered on the s -th cylinder written in the RF $_t$ turns out to be

$$\begin{aligned}
 &RW_m(2\chi_s - \xi_s, \zeta_s) \\
 &= \frac{1}{2\pi} \int_{-\infty}^{+\infty} \Gamma(n_{\parallel})F_m(\chi_s, n_{\parallel})\exp[in_{\parallel}(\zeta_t^0 - \xi_s^0)] \\
 &\quad \times \exp[in_{\perp}\chi_t]\exp(-in_{\perp}\xi_t + in_{\parallel}\zeta_t)dn_{\parallel}. \tag{17}
 \end{aligned}$$

The last exponential in this equation represents a plane wave and can be easily expressed in terms of Bessel functions centered on $R\mathcal{F}_t$ as

$$\exp(-in_{\perp}\xi_t + in_{\parallel}\zeta_t) = \sum_{l=-\infty}^{+\infty} i^l \exp(-il\bar{\psi})J_l(\rho_t)\exp(il\vartheta_t), \tag{18}$$

where $\bar{\psi} = \pi - \psi$, the angle ψ being defined as $\psi = \arcsin n_{\parallel}$, $\forall n_{\parallel} \in (-\infty, +\infty)$. Thus Eq. (17) becomes

$$\begin{aligned}
 &RW_m(2\chi_s - \xi_s, \zeta_s) \\
 &= \sum_{l=-\infty}^{+\infty} i^l J_l(\rho_t)\exp(il\vartheta_t) \frac{(-1)^l}{2\pi} \\
 &\quad \times \int_{-\infty}^{+\infty} \Gamma(n_{\parallel})F_m(\chi_s + \chi_t, n_{\parallel}) \\
 &\quad \times \exp[in_{\parallel}(\zeta_t^0 - \xi_s^0)]\exp(il \arcsin n_{\parallel})dn_{\parallel} \\
 &= \sum_{l=-\infty}^{+\infty} J_l(\rho_t)\exp(il\vartheta_t) \frac{1}{2\pi} \\
 &\quad \times \int_{-\infty}^{+\infty} \Gamma(n_{\parallel})F_{l+m}(\chi_s + \chi_t, n_{\parallel}) \\
 &\quad \times \exp[in_{\parallel}(\zeta_t^0 - \xi_s^0)]dn_{\parallel} \\
 &= \sum_{l=-\infty}^{+\infty} J_l(\rho_t)\exp(il\vartheta_t)RW_{l+m}(\chi_s + \chi_t, \zeta_t^0 - \xi_s^0), \tag{19}
 \end{aligned}$$

where use has been made of Eq. (15) and of the identity²⁵

$$\exp(i \arcsin n_{\parallel}) = i \exp(-i \arccos n_{\parallel}). \tag{20}$$

In a sense, Eq. (19) is a generalization of Graf's formula for the reflected cylindrical waves. By substituting from Eq. (19) into Eq. (14) and by interchanging indices m and l , after some algebra we can write

$$\begin{aligned}
 V_{dr}(\xi, \zeta) &= V_0 \sum_{m=-\infty}^{+\infty} J_m(\rho_t)\exp(im\vartheta_t) \\
 &\quad \times \sum_{s=1}^N \sum_{l=-\infty}^{+\infty} i^l \exp(-il\varphi)c_{sl}RW_{l+m} \\
 &\quad \times (\chi_s + \chi_t, \zeta_t^0 - \xi_s^0). \tag{21}
 \end{aligned}$$

If the cylinders are far enough from the reflecting surface, the field (21) can be neglected, because the RW_{l+m} functions vanish for large values of the first argument, as can be seen starting from their definition [see Eqs. (12) and (13)]. In the following, however, we shall not use such an approximation in our numerical results.

So far we have written all the contributions to the total field in $R\mathcal{F}_t$ ($t = 1, \dots, N$). Now we have to impose suit-

able boundary conditions on each cylindrical surface. To do this we will write the final expression of the total field $V(\xi, \zeta)$ by using Eqs. (3), (5), (11), and (21):

$$\begin{aligned}
 V(\xi, \zeta) &= V_i(\xi, \zeta) + V_r(\xi, \zeta) + V_d(\xi, \zeta) + V_{dr}(\xi, \zeta) \\
 &= V_0 \sum_{m=-\infty}^{+\infty} J_m(\rho_t)\exp(im\vartheta_t) \\
 &\quad \times \left\{ i^m \exp(-im\varphi)\exp(in_{\perp}^i \xi_t^0 + in_{\parallel}^i \zeta_t^0) \right. \\
 &\quad + i^m \exp(-im\varphi')\Gamma(n_{\parallel}^i)\exp(-in_{\parallel}^i \xi_t^0 + in_{\parallel}^i \zeta_t^0) \\
 &\quad + \sum_{s=1}^N \sum_{l=-\infty}^{+\infty} i^l \exp(-il\varphi)c_{sl} \left[CW_{l-m}(\xi_{st}, \zeta_{st}) \right. \\
 &\quad \times (1 - \delta_{st}) + RW_{l+m}(\chi_s + \chi_t, \zeta_t^0 - \xi_s^0) \\
 &\quad \left. \left. + \delta_{st} \delta_{lm} \frac{H_m^{(1)}(\rho_t)}{J_m(\rho_t)} \right] \right\}. \tag{22}
 \end{aligned}$$

In the double sum of Eq. (22), the first two terms in the square brackets take account of the cylinder-cylinder and the cylinder-interface interactions, respectively. As we remarked after Eq. (14), the importance of the former interaction term increases with the density of the scatterers, according to general considerations regarding the phenomenon of enhanced backscattering.^{20,53} The presence of the reflecting surface gives rise to the latter interaction term, which increases on reduction of the distance between the cylinders and the interface.

The boundary conditions are defined by the following equations:

$$\begin{cases} V|_{\rho_t=ka_t} = 0 & (t = 1, \dots, N) \text{ for TM polarization} \\ \partial_{\rho_t} V|_{\rho_t=ka_t} = 0 & (t = 1, \dots, N) \text{ for TE polarization} \end{cases} \tag{23}$$

By substituting from Eq. (22) into Eq. (23), after some algebra we obtain the following linear system for the unknown coefficients c_{sl}

$$\sum_{s=1}^N \sum_{l=-\infty}^{+\infty} A_{ml}^{st} c_{sl} = B_m^t, \quad \begin{cases} m = 0, \pm 1, \pm 2, \dots \\ t = 1, \dots, N \end{cases}, \tag{24}$$

where

$$A_{lm}^{st} = i^l \exp(-il\varphi) \{ [CW_{l-m}(\xi_{st}, \zeta_{st})(1 - \delta_{st}) + I_{l+m}^{st}]G_m(ka_t) + \delta_{st} \delta_{lm} \}, \tag{25a}$$

$$I_p^{st} = RW_p(\chi_s + \chi_t, \zeta_t^0 - \xi_s^0), \tag{25b}$$

$$\begin{aligned}
 B_m^t &= -i^m \exp(in_{\parallel}^i \zeta_t^0)G_m(ka_t) \\
 &\quad \times [\exp(in_{\perp}^i \xi_t^0)\exp(-im\varphi) \\
 &\quad + \Gamma(n_{\parallel}^i)\exp(-in_{\perp}^i \xi_t^0)\exp(-im\bar{\varphi})], \tag{25c}
 \end{aligned}$$

and the function $G_m(x)$, which refers to the polarization state of the field involved, is defined as²⁵

$$G_m(x) = \begin{cases} \frac{J_m(x)}{H_m^{(1)}(x)} & \text{for TM polarization} \\ \frac{J'_m(x)}{H_m^{(1)'}(x)} & \text{for TE polarization} \end{cases}, \quad (26)$$

where the prime denotes derivation.

For the quantities I_p^{st} in Eq. (25b) the following symmetry property can be derived (see Appendix A):

$$I_p^{ts} = (-1)^p I_{-p}^{st}. \quad (27)$$

It is useful to note that, if Γ is constant with respect to n_{\parallel} , the quantities (25b) can be evaluated analytically as

$$I_p^{st} = \Gamma CW_p(\chi_s + \chi_t, \zeta_t^0 - \zeta_s^0); \quad (28)$$

i.e., the V_{dr} field reduces to the field diffracted by N image cylinders placed at symmetrical positions with respect to the reflecting surface under the action of V_r as the incident field. In particular, this is the case for a perfectly conducting medium, for which $\Gamma = -1$.

After a suitable truncation of the series in Eq. (24), to be discussed in Section 3, such an equation system can be solved. Then it is possible to evaluate the electric (magnetic) field for TM (TE) polarization by means of Eqs. (2), (4), (6), and (14) everywhere outside the cylinders. In addition, the transverse-field components could be evaluated along the lines discussed in Ref. 25. In the following we focus our attention on the far-field limit, where the obtained expressions assume a very simple form.

B. Far-Field Limit

The total diffracted field can be easily computed by means of Eqs. (6) and (14),

$$\begin{aligned} V_d^{\text{tot}}(\xi, \zeta) &= V_d(\xi, \zeta) + V_{dr}(\xi, \zeta) \\ &= V_0 \sum_{s=1}^N \sum_{m=-\infty}^{+\infty} \hat{c}_{sm} [CW_m(\xi_s, \zeta_s) \\ &\quad + RW_m(2\chi_s - \xi_s, \zeta_s)], \end{aligned} \quad (29)$$

where for the sake of compactness, coefficients

$$\hat{c}_{sm} = i^m \exp(-im\varphi) c_{sm} \quad (30)$$

have been introduced. With reference to the notation shown in Fig. 2, in the far-field limit, taking account of the asymptotic expansion of cylindrical functions,^{25,54}

$$CW_m(\xi_s, \zeta_s) \approx \left(\frac{-2i}{\pi\rho_s}\right)^{1/2} i^{-m} \exp(i\rho_s) \exp(im\vartheta_s), \quad (31a)$$

$$\begin{aligned} RW_m(2\chi_s - \xi_s, \zeta_s) &\approx \left(\frac{-2i}{\pi\bar{\rho}_s}\right)^{1/2} \Gamma(\sin\bar{\vartheta}_s) i^{-m} \\ &\quad \times \exp(i\bar{\rho}_s) \exp(im\bar{\vartheta}_s), \end{aligned} \quad (31b)$$

and considering the following approximations,

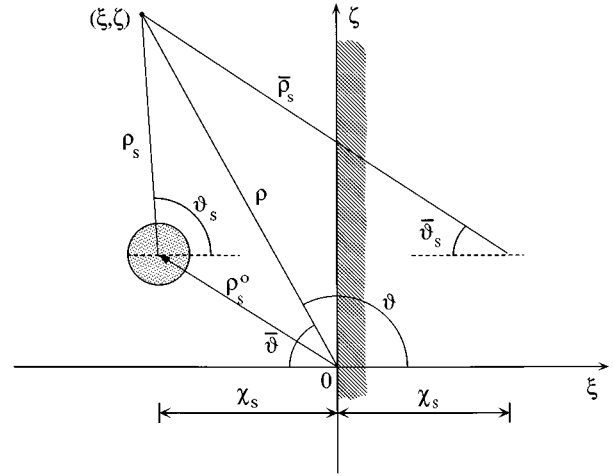


Fig. 2. Geometry for the far-field analysis.

$$\frac{1}{\bar{\rho}_s} \approx \frac{1}{\rho_s} \approx \frac{1}{\rho}, \quad \vartheta_s \approx \vartheta, \quad \bar{\vartheta}_s \approx \pi - \vartheta,$$

$$\begin{aligned} \exp(i\rho_s) &\approx \exp(i\rho) \exp(i\chi_s \cos \vartheta - i\zeta_s^0 \sin \vartheta), \\ \exp(i\bar{\rho}_s) &\approx \exp(i\rho) \exp(-i\chi_s \cos \vartheta - i\zeta_s^0 \sin \vartheta), \end{aligned} \quad (32)$$

Eq. (29) becomes

$$V_d^{\text{tot}}(\xi, \zeta) \approx V_0 \left(\frac{-2i}{\pi\rho}\right)^{1/2} \exp(i\rho) g(\vartheta), \quad (33)$$

where the function

$$\begin{aligned} g(\vartheta) &= \sum_{s=1}^N \sum_{m=-\infty}^{+\infty} i^{-m} \hat{c}_{sm} \exp(i\chi_s \cos \vartheta - i\zeta_s^0 \sin \vartheta) \\ &\quad \times [\exp(im\vartheta) + (-1)^m \Gamma(\sin \vartheta) \\ &\quad \times \exp(-i2\chi_s \cos \vartheta) \exp(-im\vartheta)] \end{aligned} \quad (34)$$

represents the angular far-field radiation pattern.

3. NUMERICAL RESULTS

Equations (24) and (25) solve in a rigorous way the plane-wave scattering problem for N perfectly conducting circular cylinders placed near a plane interface with general reflection properties. However, although no approximations have been introduced in the theoretical basis of the method, in order to implement it we unavoidably have to truncate the series in Eq. (24). Physically, this means that the field diffracted by the s th cylinder will be expressed by a finite sum of CW_m functions [see Eq. (6)], letting m run from $-M_s$ to M_s , M_s being the truncation order for the s th cylinder. The dimension of the resolving linear system in Eq. (24) turns out to be

$$\sum_{s=1}^N (2M_s + 1) = N + 2 \sum_{s=1}^N M_s. \quad (35)$$

As a matter of fact, M_s depends on the size of the s th cylinder,⁴⁹ and therefore the algorithm complexity grows with the size and the number of cylinders. In order to give a quantitative criterion for choosing M_s , we per-

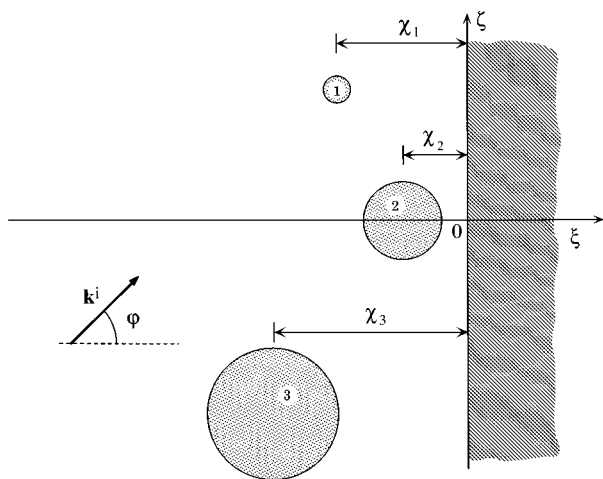


Fig. 3. Scattering configuration used for the convergence test: $N = 3$; $ka_1 = 1$, $\chi_1 = 10$, $\zeta_1 = 10$; $ka_2 = 3$, $\chi_2 = 5$, $\zeta_2 = 0$; $ka_3 = 5$, $\chi_3 = 15$, $\zeta_3 = -15$. The refractive index of the dielectric medium is $n = 1.5$, and the incidence angle of the impinging plane wave is $\varphi = 45^\circ$.

formed several numerical tests for both the TM and the TE polarization states. Figure 3 shows the geometrical layout corresponding to a typical convergence test: Three cylinders, with $ka_1 = 1$, $ka_2 = 3$, $ka_3 = 5$, are placed at distances $\chi_1 = 10$, $\chi_2 = 5$, and $\chi_3 = 15$ from the reflecting surface. The latter is a vacuum-dielectric interface, whence the reflecting coefficient $\Gamma(n_{||})$ is given by the well-known Fresnel formulas. The ζ coordinates of the three cylinders are $\zeta_1 = 10$, $\zeta_2 = 0$, and $\zeta_3 = -15$. The refractive index of the dielectric medium is $n = 1.5$, and the incidence angle of the plane wave is $\varphi = 45^\circ$. As suggested in Refs. 15–17, we set $M_s = \mu ka_s$ ($s = 1, 2, 3$), μ being an integer factor. Figure 4 shows the behavior of the modulus of the expansion coefficients c_{sm} for all cylinders for $\mu = 1, 2, 3, 4$, for (a) TM and (b) TE polarization.

It can be seen that the coefficients tend to stabilize when μ exceeds 2, and the same behavior has been observed in most cases, so that the well-known rule^{15,16} suggesting the choice $\mu = 3$ seems to be a reasonable compromise between accuracy and computational cum-

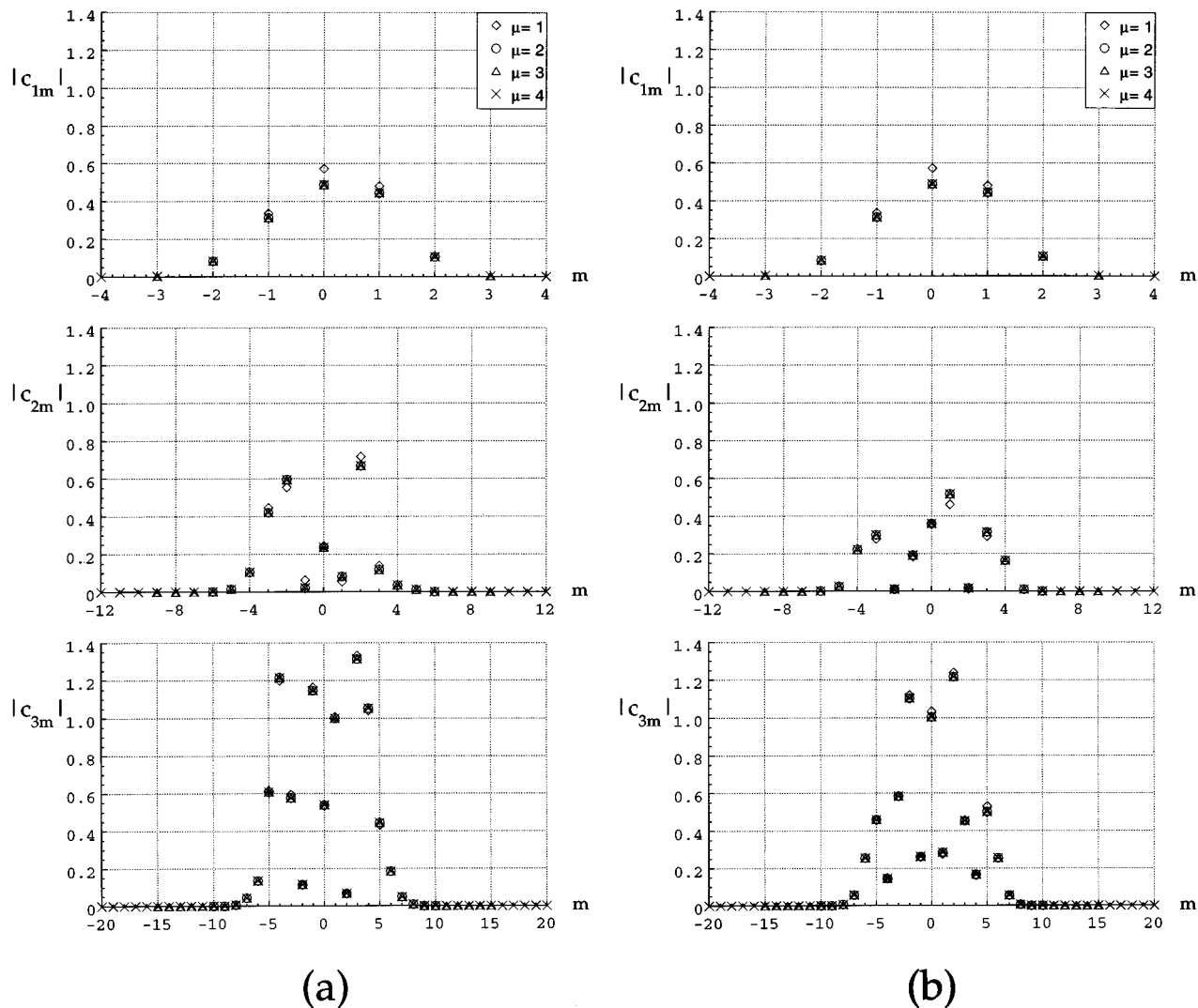


Fig. 4. Behavior of the modulus of the expansion coefficients c_{sm} for the configuration illustrated in Fig. 3 for increasing values of the truncation order $M_s = \mu ka_s$ for (a) TM and (b) TE polarization ($s = 1, 2, 3$; $m = -M_s, \dots, M_s$).

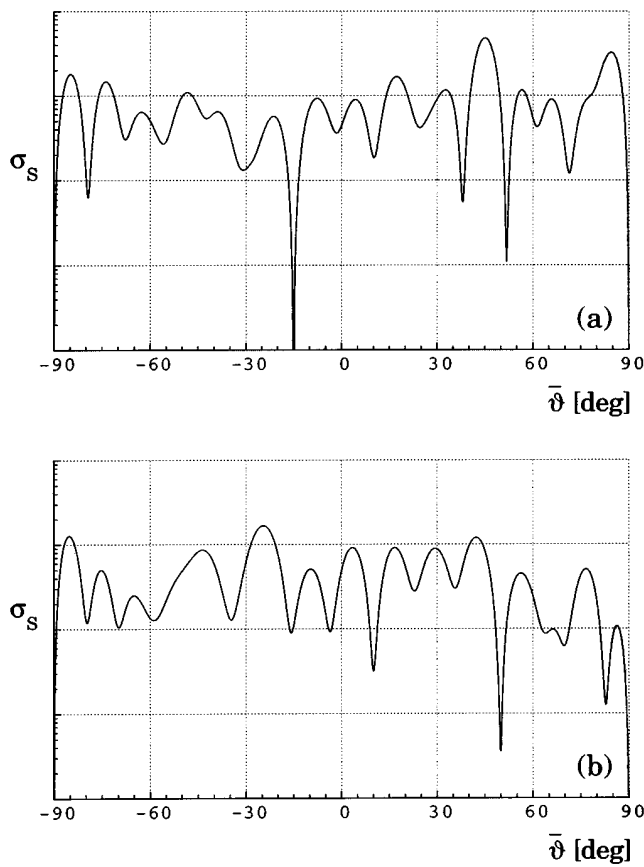


Fig. 5. Semilogarithmic plot [arbitrary units (a.u.)] of the scattering cross section σ_S as a function of the scattering angle $\bar{\vartheta}$ for the configuration illustrated in Fig. 3, for (a) TM and (b) TE polarization. $\varphi = 45^\circ$, $n = 1.5$.

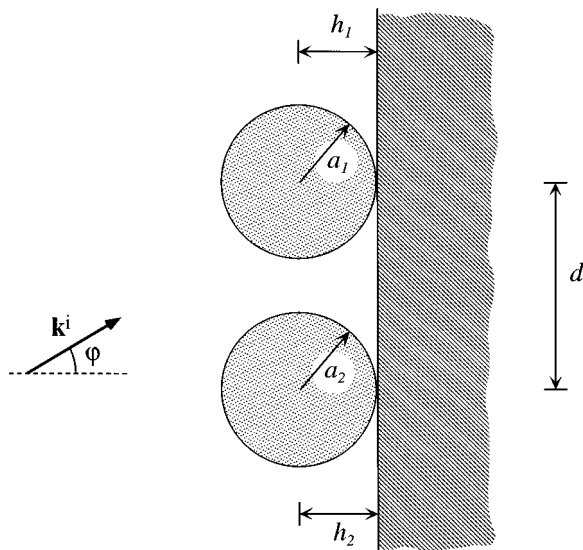


Fig. 6. Geometrical layout for the study of two interacting cylinders on a perfect mirror.

bersomeness. It should be stressed, however, that for some particular situations, especially for small cylinder-interface distances in TE polarization, convergence is achieved with values of μ up to 4 or 5. In Fig. 5 we show

the scattering cross section⁵⁵ σ_S for the test case of Fig. 3 as a function of the scattering angle $\bar{\vartheta} = \pi - \vartheta$ (see Fig. 2), for (a) TM and (b) TE polarization.

We shall now illustrate the main computational advantages and limitations of the proposed method. An important problem to be considered is the numerical evaluation of the matrix elements I_{l+m}^{st} [see Eqs. (25a) and (25b)], which actually represents the most limiting factor of the present method, at least from a merely computational point of view. Indeed, these functions are defined by means of integrals of oscillating functions, whose amplitude and frequency depend strongly on the order $l + m$ and on the mutual distances $\zeta_t^0 - \zeta_s^0$ ($s, t = 1, 2, \dots, N$), respectively.

As shown above, the maximum value of $l + m$ is related to the radius of the cylinders, and the transverse (i.e., in the ζ direction) extension of the whole diffractive structure fixes the maximum value of $\zeta_t^0 - \zeta_s^0$. High values of $l + m$ or $\zeta_t^0 - \zeta_s^0$ make the evaluation of the involved integrals rather cumbersome, and special integration routines based on a combined use of Gaussian techniques and extrapolation methods have been developed.⁵⁶ We tested the algorithm for values of M_s up to some tens, corresponding to cylinders whose diameters are of the order of some wavelengths. It should be stressed that in such cases neither the Rayleigh nor the

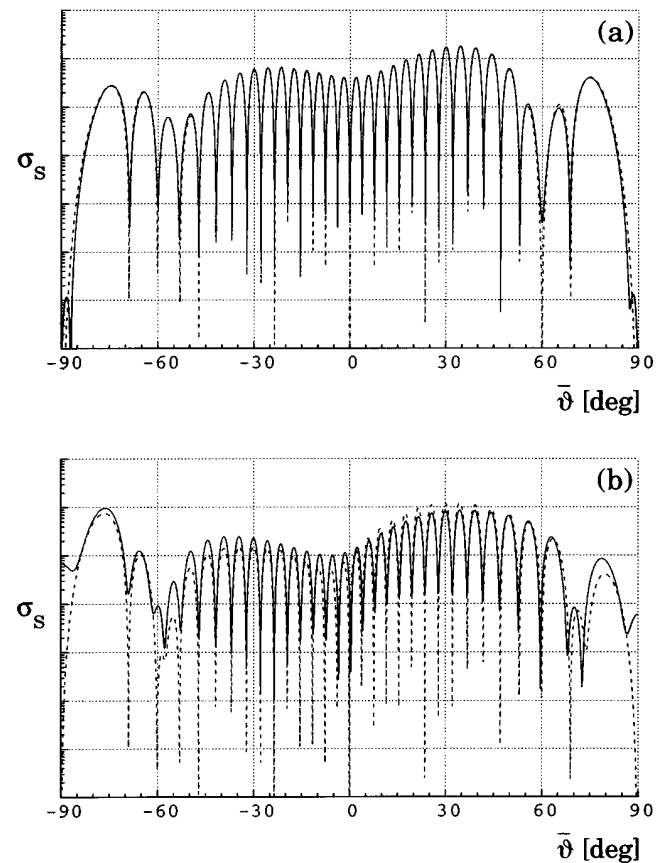


Fig. 7. Semilogarithmic plot (a.u.) of the scattering cross section σ_S as a function of the scattering angle $\bar{\vartheta}$ for the configuration illustrated in Fig. 6, for (a) TM and (b) TE polarization. $ka = \pi$, $kh = \pi$, $\varphi = 30^\circ$, $kd = 30ka$.

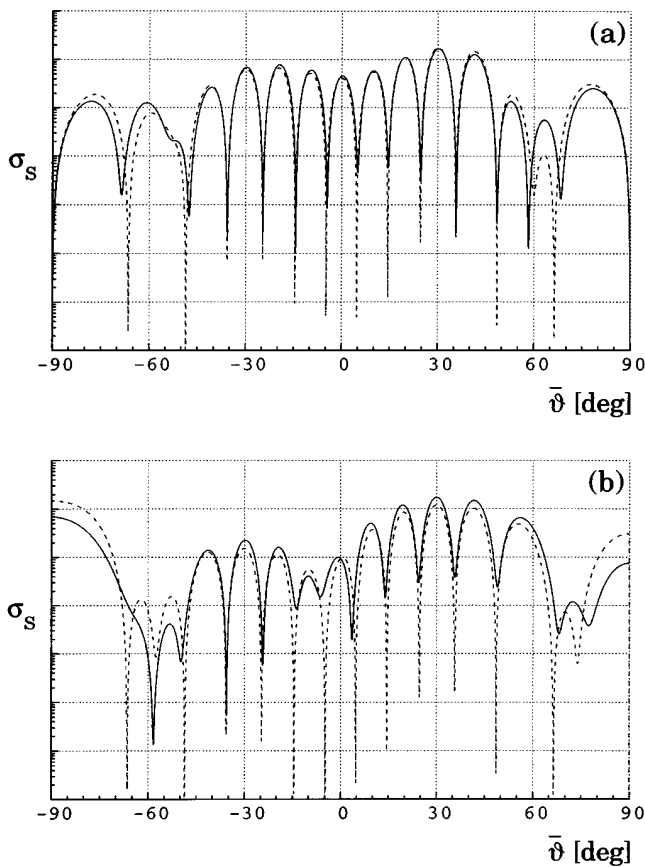


Fig. 8. Same as in Fig. 7, except that $kd = 12ka$.

Kirchhoff approximation (valid for very small or very large objects, respectively) can be used. To give an idea of the execution time, we report that the calculation of the 2000-point plots of Fig. 5 requires ~ 20 s on a HP-9000 Apollo workstation, with use of a FORTRAN code.

In next subsections we present two examples of typical problems with which our method can be profitably used. The first example concerns the interaction between two cylinders lying on a reflecting surface; the second one illustrates some scattering properties of a finite array of cylinders near a dielectric interface.

A. Study of the Mutual Interaction of Two Cylinders on a Mirror

The study of multiple scattering by two objects has been the subject of several studies.^{10,11,13,22} As we pointed out in Section 1, a large part of them dealt with scatterers in a homogeneous medium, but it is not easy to find similar studies for the case of a plane of discontinuity placed near the scatterers. Quite recently⁵⁷ Valle *et al.* presented some numerical results for the case of two perfectly conducting circular cylinders placed onto a perfectly conducting flat substrate. The diffractive structure was illuminated by a Gaussian beam, because their numerical method, based on the extinction theorem, treats surfaces of finite extension. In their case the diameter of the two cylinders was equal to the wavelength, corresponding to $ka_1 = ka_2 = \pi$, and cylinders were in contact with the

surface, i.e., $kh_1 = kh_2 = \pi$; the incidence angle of the impinging field was $\varphi = 30^\circ$. Figure 6 depicts the geometry of the problem.

As pointed out in Ref. 57, such geometry is quite useful to illustrate the physics of the interaction between the two cylinders. The far-field pattern, indeed, is generated by the interference of the fields diffracted by each cylinder, as in a Young two-slit interferometer. So, if the two cylinders were noninteracting, the far-field diffracted intensity would be simply given by four times the intensity diffracted by a single cylinder, multiplied by the function $\cos^2 \delta(\bar{\vartheta})$, where $\delta(\bar{\vartheta}) = kd/2 (\sin \bar{\vartheta} - \sin \varphi)$,⁵⁷ kd denoting the distance between the axes of the cylinders.

When the scatterers are far enough from each other so that the mutual interaction can be neglected, the total far-field diffracted intensity must look like the one obtained by noninteracting cylinders, but the resemblance is reduced as the distance kd decreases. Such behavior is shown in Fig. 7 ($kd = 30\pi$), Fig. 8 ($kd = 12\pi$), and Fig. 9 ($kd = 4\pi$), for (a) TM and (b) TE polarization. In these figures the corresponding pattern for noninteracting cylinders is shown, too (dashed curves). It can be seen that, in general, the range of kd values for which the interaction is not negligible is considerably wider for TE than for TM polarization. This is essentially because for TM polarization, boundary conditions force the electric field to vanish on the mirror surface, whereas this is not true for TE polarization, for which the magnetic field is to be considered. This, in turn, implies that the field radi-

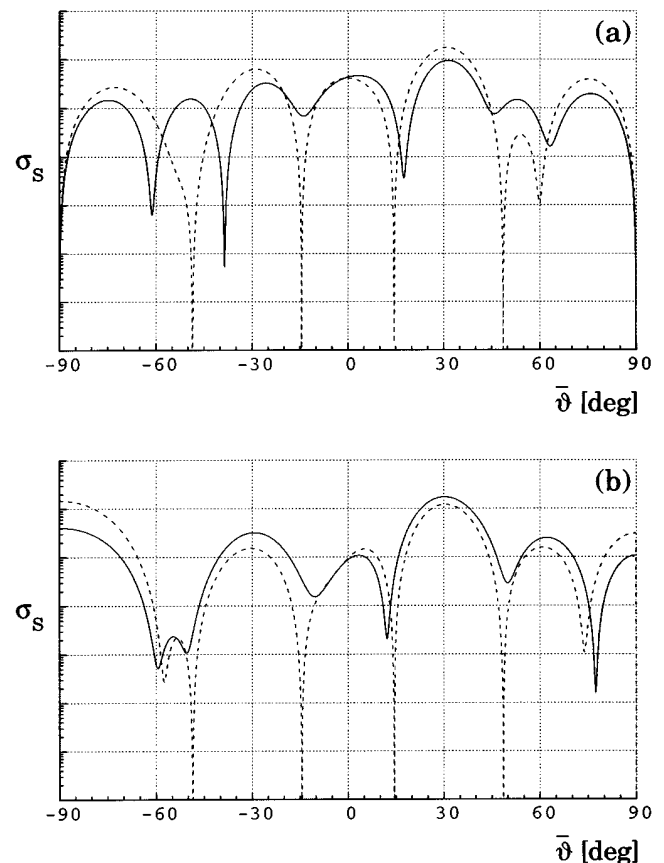


Fig. 9. Same as in Fig. 7, except that $kd = 4ka$.

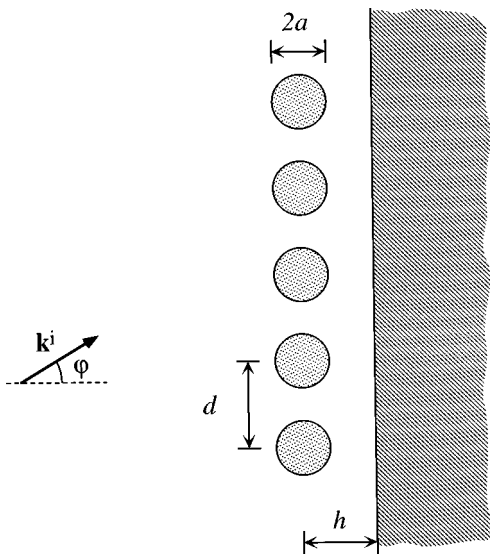


Fig. 10. A finite grating parallel to the interface.

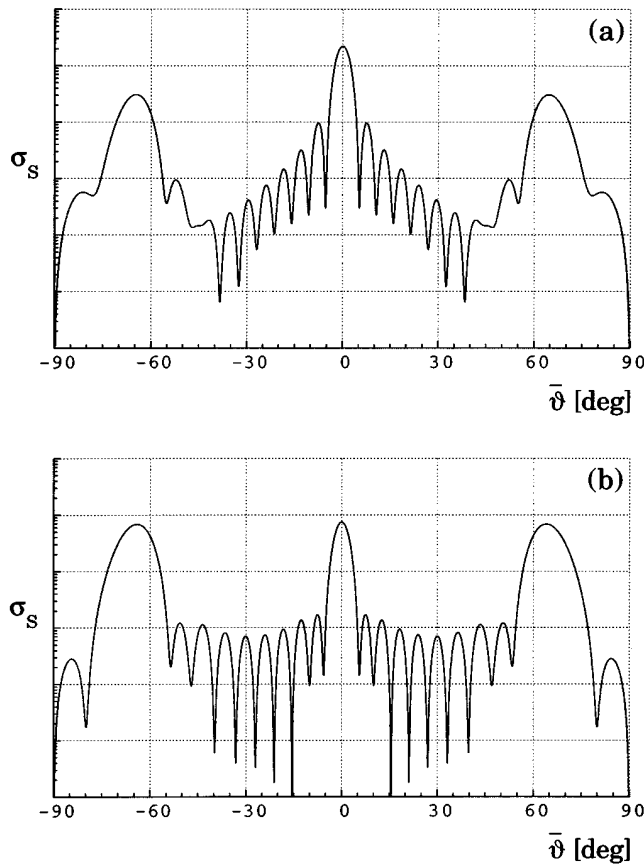


Fig. 11. Semilogarithmic plot (a.u.) of the scattering cross section σ_S as a function of the scattering angle ϑ for an optical grill placed near a vacuum–dielectric interface (see Fig. 10). $n = 2$, $\varphi = 0^\circ$, $N = 10$, $ka = 1.0$, $kh = 3.0$, $kd = 7.0$, for (a) TM and (b) TE polarization.

ated by each cylinder (together with its image) and reaching the other cylinder is smaller for TM than for TE polarization.

The cases of Figs. 8 and 9 correspond exactly to those of Figs. 2 and 3 of Ref. 57 except that a different incident beam and a finite reflecting surface are considered there. Taking into account the differences between the two models, our results show quite good agreement.

B. Study of Finite Diffraction Gratings

A particular arrangement of cylinders whose scattering properties can be studied with the present approach is a finite diffraction grating. It consists of N equidistant equal cylinders whose axes lie on a plane parallel to the reflecting surface (see Fig. 10). This structure is of considerable importance in optics and microwaves. In particular, such a configuration turns out to be useful for applications in plasma physics^{45,46} as well as in the study of some aspects of light–matter interaction such as enhanced backscattering⁵³ and surface–polariton interaction.⁵⁸

Figures 11–13 show the scattering cross section σ_S as a function of the scattering angle $\bar{\vartheta}$ for a finite diffraction grating of $N = 10$ cylinders placed in front of a vacuum–dielectric interface with refractive index $n = 2.0$. The period of the grating is $kd = 7.0$, the other parameters being $ka = 1.0$, $kh = 3.0$, $\varphi = 0^\circ$ (Fig. 11), $\varphi = 30^\circ$ (Fig. 12), and $\varphi = 60^\circ$ (Fig. 13). TM (a) and TE (b) polarization states are depicted, and the refractive index is chosen so as to give rise to an appreciable reflection.

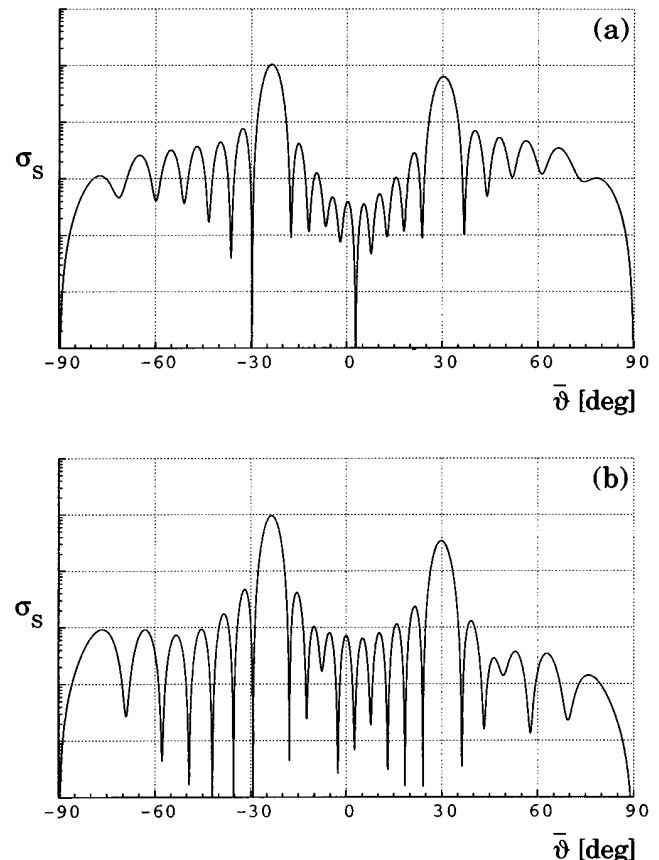


Fig. 12. Same as in Fig. 11, except that $\varphi = 30^\circ$.

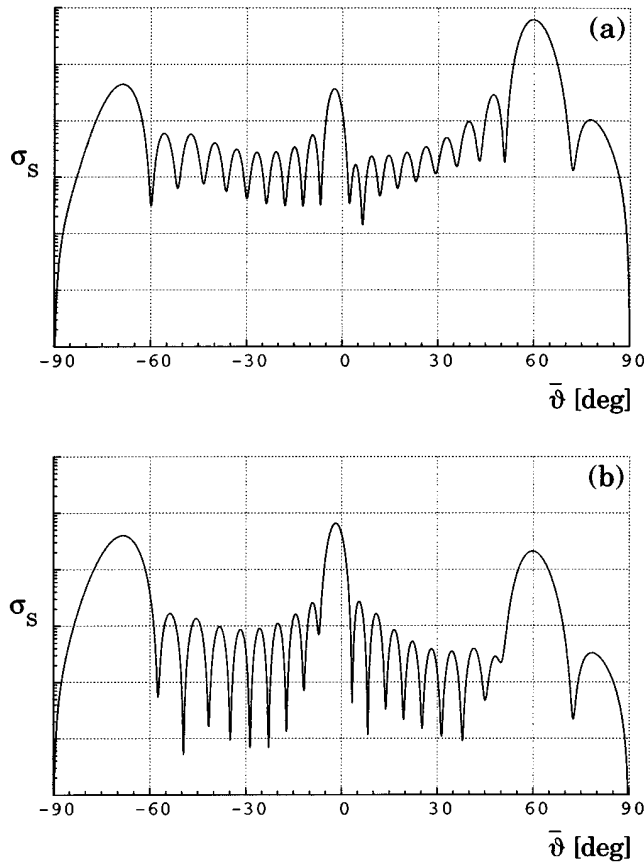


Fig. 13. Same as in Fig. 11, except that $\varphi = 60^\circ$.

In these figures, peaks can be observed at the angles $\bar{\vartheta}_m$ defined as

$$\sin \bar{\vartheta}_m = -\sin \varphi + m \frac{2\pi}{kd} \quad (m = 0, \pm 1, \pm 2, \dots), \quad (36)$$

corresponding to the propagation directions of the diffracted orders.⁵⁹ In particular, for normal incidence, i.e., $\varphi = 0^\circ$, diffraction orders with $m = 0$ and $m = \pm 1$ are present, the other ones being evanescent. On the contrary, for $\varphi = 30^\circ$ the order $m = 1$ becomes evanescent, so that only the orders $m = 0$ and $m = -1$ can be seen. For $\varphi = 60^\circ$ the order $m = -2$ becomes homogeneous and appears in the far-field pattern. As is known, the nonzero width of the peaks is related to the finite extension of the grating. This can be seen by comparing Fig. 13 with Fig. 14, where the same parameters have been used, but in the latter case the number of cylinders is set to $N = 20$, corresponding to a total extension that is twice the previous one.

4. CONCLUSIONS

We have presented here an efficient method to treat the problem of the plane-wave scattering by N perfectly conducting circular cylinders in the presence of a plane of discontinuity for the optical constants. The method, based on the plane-wave spectrum of cylindrical functions, allows the scattering problem to be tackled for a

wide class of discontinuity surfaces (such as dielectric or metallic interfaces, multilayered structures, and anisotropic and lossy media) and for arbitrary sets of cylinders, in both TM and TE polarization states.

Following analogous lines, the case of circular cylinders characterized by a complex dielectric constant could be treated as well, allowing, in particular, the interesting case of real conductors to be studied. Such an extension could be quite useful, because in the high-frequency limit, especially for TE polarization, the approximation of perfect conductors may show lack of validity.

The method has been tested for several geometrical configurations, showing good convergence properties, computational efficiency, and high reliability. In particular, we have shown that the method can be profitably used in studying some typical scattering problems, such as cylinder-cylinder interaction and diffraction by finite gratings in the presence of a reflecting plane. Our approach seems to be promising also for other applications, such as antenna analysis and design, detection of defects in semiconductors,^{42,43} and near-field optics²⁹ and, with suitable extensions, scattering by dielectric, possibly lossy, cylinders on substrates.^{21,27} Moreover, it can be applied to the modeling of arbitrary shaped cylindrical scatterers by means of a suitable arrangement of circular cylinders, following the lines suggested in Refs. 40 and 41.

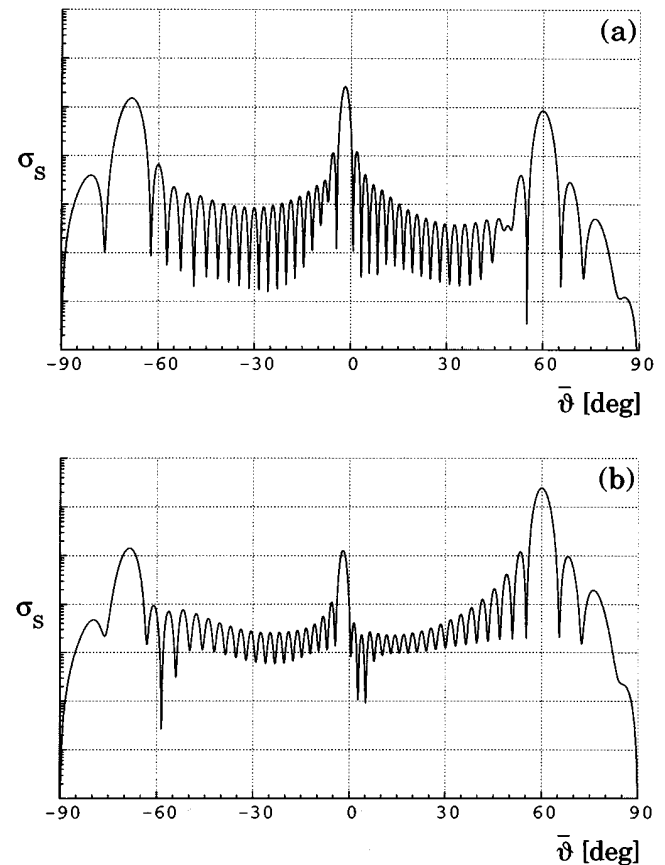


Fig. 14. Semilogarithmic plot (a.u.) of the scattering cross section σ_S as a function of the scattering angle $\bar{\vartheta}$ for the case shown in Fig. 13, except that $N = 20$, for (a) TM and (b) TE polarization.

APPENDIX A

Starting from Eq. (25b), and recalling Eq. (25a), we have for I_p^{ts} the following expression:

$$\begin{aligned}
 I_p^{ts} &= \text{RW}_p(\chi_t + \chi_s, \zeta_s^0 - \zeta_t^0) \\
 &= \frac{1}{2\pi} \int_{-\infty}^{+\infty} \Gamma(n_{\parallel}) F_p(\chi_t + \chi_s, n_{\parallel}) \\
 &\quad \times \exp[in_{\parallel}(\zeta_s^0 - \zeta_t^0)] dn_{\parallel} \\
 &= \frac{1}{2\pi} \int_{-\infty}^{+\infty} \Gamma(n_{\parallel}) F_p(\chi_t + \chi_s, n_{\parallel}) \\
 &\quad \times \exp[-in_{\parallel}(\zeta_t^0 - \zeta_s^0)] dn_{\parallel} \\
 &= \frac{1}{2\pi} \int_{-\infty}^{+\infty} \Gamma(-n_{\parallel}) F_p(\chi_s + \chi_t, -n_{\parallel}) \\
 &\quad \times \exp[in_{\parallel}(\zeta_t^0 - \zeta_s^0)] dn_{\parallel} \\
 &= \frac{1}{2\pi} \int_{-\infty}^{+\infty} \Gamma(n_{\parallel}) (-1)^p F_{-p}(\chi_s + \chi_t, n_{\parallel}) \\
 &\quad \times \exp[in_{\parallel}(\zeta_t^0 - \zeta_s^0)] dn_{\parallel} = (-1)^p I_{-p}^{st}, \quad (\text{A1})
 \end{aligned}$$

where use has been made of the parity of the function $\Gamma(n_{\parallel})$ and of the following relation of functions F_p :

$$F_p(\chi, -n_{\parallel}) = (-1)^p F_{-p}(\chi, n_{\parallel}). \quad (\text{A2})$$

The last equality in Eq. (A1) coincides with Eq. (27).

ACKNOWLEDGMENTS

The present work is supported by Ministero dell'Università e della Ricerca Scientifica e Tecnologica and by Istituto Nazionale di Fisica della Materia.

REFERENCES

- W. Von Ignatowsky, "Zur theorie der Gitter," *Ann. Physik* **44**, 369–436 (1914).
- V. Twersky, "On scattering of waves by an infinite grating of circular cylinders," *IRE Trans. Antennas Propag.* **AP-10**, 737–765 (1962).
- W. Wasylkiwskyj, "On the transmission coefficient of an infinite grating of parallel perfectly conducting circular cylinders," *IEEE Trans. Antennas Propag.* **AP-19**, 704–708 (1971).
- J. R. Wait, "Reflection at arbitrary incidence from a parallel wire grid," *Appl. Sci. Res. B* **4**, 393–400 (1954).
- J. H. Richmond, "Scattering by an arbitrary array of parallel wires," *IEEE Trans. Microwave Theory Tech.* **MTT-13**, 408–412 (1965).
- L. O. Wilson, "The shielding of a plane wave by a cylindrical array of infinitely thin wires," *IEEE Trans. Antennas Propag.* **AP-22**, 689–696 (1974).
- R. Vescovo, "Electromagnetic scattering from cylindrical arrays of infinitely long thin wires," *Electron. Lett.* **31**, 1646–1647 (1995).
- A. C. Ludwig, "Wire grid modeling of surfaces," *IEEE Trans. Antennas Propag.* **AP-35**, 1045–1048 (1987).
- R. J. Paknys, "The near field of a wire grid model," *IEEE Trans. Antennas Propag.* **39**, 994–999 (1991).
- G. O. Olaofe, "Scattering by two cylinders," *Radio Sci.* **5**, 1351–1360 (1970).
- K. Hongo, "Multiple scattering by two conducting circular cylinders," *IEEE Trans. Antennas Propag.* **AP-26**, 748–751 (1978).
- A. Z. Elsherbeni and M. Hamid, "Scattering by parallel conducting circular cylinders," *IEEE Trans. Antennas Propag.* **AP-35**, 355–358 (1987).
- V. Twersky, "Multiple scattering of radiation by an arbitrary configuration of parallel cylinders," *J. Acoust. Soc. Am.* **24**, 42–46 (1952).
- N. Zitron and S. N. Karp, "Higher-order approximations in multiple scattering. Two-dimensional scalar case," *J. Math. Phys.* **2**, 394–406 (1961).
- H. A. Ragheb and M. Hamid, "Scattering by N parallel conducting circular cylinders," *Int. J. Electron.* **59**, 407–421 (1985).
- A. Z. Elsherbeni, "A comparative study of two-dimensional multiple scattering techniques," *Radio Sci.* **29**, 1023–1033 (1994).
- D. R. Wilton and R. Mittra, "A new numerical approach to the calculation of electromagnetic scattering properties of two-dimensional bodies of arbitrary cross section," *IEEE Trans. Antennas Propag.* **AP-20**, 310–317 (1972).
- H. A. Kalthor and Armand, "Scattering of waves by gratings of conducting cylinders," *Proc. IEE* **122**, 245–248 (1975).
- F. Zolla, R. Petit, and M. Cadilhac, "Electromagnetic theory of diffraction by a system of parallel rods: the method of fictitious sources," *J. Opt. Soc. Am. A* **11**, 1087–1096 (1994).
- D. Felbacq, G. Tayreb, and D. Maystre, "Scattering by a random set of parallel cylinders," *J. Opt. Soc. Am. A* **11**, 2526–2538 (1994).
- B. Schlicht, K. F. Wall, R. K. Chang, and P. W. Barber, "Light scattering by two parallel glass fibers," *J. Opt. Soc. Am. A* **4**, 800–809 (1987).
- T. G. Tsuei and P. W. Barber, "Multiple scattering by two parallel dielectric cylinders," *Appl. Opt.* **27**, 3375–3381 (1988).
- J. R. Wait, "Reflection from a wire grid parallel to a conducting plane," *Can. J. Phys.* **32**, 571–579 (1954).
- J. R. Wait, "The impedance of a wire grid parallel to a dielectric interface," *IRE Trans. Microwave Theory Tech.* **5**, 99–102 (1957).
- R. Borghi, F. Frezza, F. Gori, M. Santarsiero, and G. Schettini, "Plane-wave scattering by a perfectly conducting circular cylinder near a plane surface: cylindrical-wave approach," *J. Opt. Soc. Am. A* **13**, 483–493 (1996).
- P. G. Cottis and J. D. Kanellopoulos, "Scattering from a conducting cylinder above a lossy medium," *Int. J. Electron.* **65**, 1031–1038 (1988).
- M. A. Taubenblatt, "Light scattering from cylindrical structures on surfaces," *Opt. Lett.* **15**, 255–257 (1990).
- P. J. Valle, F. González, and F. Moreno, "Electromagnetic wave scattering from conducting cylindrical structures on flat substrates: study by means of the extinction theorem," *Appl. Opt.* **33**, 512–523 (1994).
- P. J. Valle, F. Moreno, J. M. Saiz, and F. González, "Near-field scattering from subwavelength metallic protuberances on conducting flat substrates," *Phys. Rev. B* **51**, 13681–13690 (1995).
- A. Madrazo and M. Nieto-Vesperinas, "Scattering of electromagnetic waves from a cylinder in front of a conducting plane," *J. Opt. Soc. Am. A* **12**, 1298–1309 (1995).
- K. B. Nahm and W. L. Wolfe, "Light scattering for spheres on a conducting plane: comparison with experiment," *Appl. Opt.* **26**, 2995–2999 (1987).
- I. V. Lindell, A. H. Sihlova, K. O. Muinonen, and P. W. Barber, "Scattering by a small object close to an interface. I. Exact-image theory formulation," *J. Opt. Soc. Am. A* **8**, 472–476 (1991).
- M. A. Taubenblatt and T. K. Tran, "Calculation of light scattering from particles and structures on a surface by the coupled-dipole method," *J. Opt. Soc. Am. A* **10**, 912–919 (1993).
- F. Moreno, F. González, J. M. Saiz, P. J. Valle, and D. L. Jordan, "Experimental study of copolarized light scattering by spherical metallic particles on conducting flat substrates," *J. Opt. Soc. Am. A* **10**, 141–157 (1993).

35. J. R. Wait, "Note on solution for scattering from parallel wires in an interface," *J. Electromagn. Waves Appl.* **4**, 1151–1155 (1990).
36. T. C. Rao and R. Barakat, "Plane wave scattering by a finite array of conducting cylinders partially buried in a ground plane: TM polarization," *Pure Appl. Opt.* **3**, 1023–1048 (1994).
37. R. Ulrich, T. J. Bridges, and M. A. Pollack, "Variable metal mesh coupler for far infrared lasers," *Appl. Opt.* **9**, 2511–2516 (1970).
38. A. Sentz, M. Pyee, C. Gastaud, J. Auvray, and J. P. Letur, "Construction of parallel grids acting as semitransparent flat mirrors in the far infrared," *Rev. Sci. Instrum.* **49**, 926–927 (1978).
39. A. Dipace, A. Doria, G. P. Gallerano, M. F. Kimmit, P. Raimondi, A. Renieri, and E. Sabia, "Compact free electron laser resonators utilizing electron transparent mirrors," *IEEE J. Quantum Electron.* **27**, 2629–2635 (1991).
40. H. A. Ragheb and M. Hamid, "Simulation of a cylindrical reflector by conducting circular cylinders," *IEEE Trans. Antennas Propag.* **AP-35**, 349–353 (1987).
41. A. Z. Elsherbeni and A. A. Kishk, "Modeling of cylindrical objects by circular dielectric and conducting cylinders," *IEEE Trans. Antennas Propag.* **40**, 96–99 (1992).
42. G. L. Wojcik, D. K. Vaughn, and L. K. Galbraith, "Calculation of light scatter from structures on silicon surfaces," in *Lasers in Microlithography*, J. S. Batchelder, O. J. Enrlich, and J. Y. Tsao, eds., *Proc. SPIE* **774**, 21–31 (1987).
43. A. J. Pidduck, D. J. Robbins, I. M. Young, A. G. Cullis, and A. R. S. Martin, "The formation of dislocations and their *in-situ* detection during silicon vapor phase epitaxy at reduced temperature," *Mater. Sci. Eng. B* **4**, 417–422 (1989).
44. M. I. Petelin and E. V. Suvorov, "Quasi optical grill for excitation of lower hybrid wave in a toroidal plasma," *Sov. Tech. Phys. Lett.* **15**, 882–886 (1989).
45. F. Frezza, F. Gori, M. Santarsiero, F. Santini, and G. Schettini, "Quasi-optical launchers for lower hybrid waves: a full-wave approach," *Nucl. Fusion* **34**, 1239–1246 (1994).
46. F. Frezza, G. Gerosa, F. Gori, M. Santarsiero, F. Santini, G. Schettini, and M. Sgroi, "Gaussian beam diffraction by a quasi-optical grating for coupling to lower-hybrid plasma waves," *Int. J. Infrared Mill. Waves* **16**, 1009–1024 (1995).
47. M. Abramowitz and I. Stegun, *Handbook of Mathematical Functions* (Dover, New York, 1972), Chap. 9, p. 358.
48. M. Abramowitz and I. Stegun, *Handbook of Mathematical Functions* (Dover, New York, 1972), Chap. 9, p. 363.
49. T. B. Senior and P. L. E. Uslenghi, "The circular cylinder," in *Electromagnetic and Acoustic Scattering by Simple Shapes*, J. J. Bowman, T. B. Senior, and P. L. E. Uslenghi, eds. (Hemisphere, New York, 1987), Chap. 2, p. 93.
50. M. Abramowitz and I. Stegun, *Handbook of Mathematical Functions* (Dover, New York, 1972), Chap. 9, p. 364.
51. M. Born and E. Wolf, *Principles of Optics*, 6th ed. (Pergamon, Oxford, 1980), Chap. 1, p. 36.
52. G. Cincotti, F. Gori, M. Santarsiero, F. Frezza, F. Furnò, and G. Schettini, "Plane wave expansion of cylindrical functions," *Opt. Commun.* **95**, 192–198 (1993).
53. M. Nieto-Vesperinas and J. C. Dainty, eds., *Scattering in Volumes and Surfaces* (North-Holland, Amsterdam, 1991).
54. W. Wang, R. Simon, and E. Wolf, "Changes in the coherence and spectral properties of partially coherent light reflected from a dielectric slab," *J. Opt. Soc. Am. A* **9**, 287–297 (1992).
55. J. J. Bowman, T. B. Senior, and P. L. E. Uslenghi, *Electromagnetic and Acoustic Scattering by Simple Shapes* (Hemisphere, New York, 1987), p. 7.
56. P. F. Davis and P. Rabinowitz, *Methods of Numerical Integration* (Academic, New York, 1984), Chap. 3.
57. P. J. Valle, F. Moreno, J. M. Saiz, and F. González, "Electromagnetic interaction between two parallel circular cylinders on a planar interface," *IEEE Trans. Antennas Propag.* **44**, 321–325 (1996).
58. A. Madrazo and M. Nieto-Vesperinas, "Surface structure and polariton interactions in the scattering of electromagnetic waves from a cylinder in front of a conducting grating: theory for the reflection photon scanning tunneling microscope," *J. Opt. Soc. Am. A* **13**, 785–795 (1996).
59. R. Petit, ed., *Electromagnetic Theory of Gratings* (Springer-Verlag, Berlin, 1980).